

Slow Magnetic Relaxation in a $\text{Co}^{\text{II}}\text{-Y}^{\text{III}}$ Single-Ion Magnet with Positive Axial Zero-Field Splitting**

Enrique Colacio,* José Ruiz, Eliseo Ruiz, Eduard Cremades, J. Krzystek, Stefano Carretta, Joan Cano, Tatiana Guidi, Wolfgang Wernsdorfer, and Euan K. Brechin*

Dedicated to Professor Reijo Sillanpää

With the discovery of molecular complexes exhibiting slow relaxation of the magnetization and magnetic hysteresis at low temperature, research activity in the field of molecular magnetism based on coordination compounds has experienced spectacular growth.^[1] These nanomagnets, called single-molecule magnets (SMMs),^[1–3] straddle the quantum/classical interface showing quantum effects, such as quantum tunneling of the magnetization and quantum phase interference, and have potential applications in molecular spintronics, ultra-high density magnetic information storage, and quantum computing at the molecular level.^[3] The motivation of much of this research activity has been provided by the prospect of integrating SMMs into nanosized devices. The origin of the SMM behavior is the existence of an energy barrier that prevents reversal of the molecular magnetization,^[1] although the currently observed energy barriers are (relatively) low and therefore SMMs act as magnets only at very low temperature. To increase the height of the energy barrier and therefore to improve the SMM properties, systems with large spin-ground states and/or with large magnetic anisotropy are required. The early examples of SMMs were clusters of transition metal ions,^[2] but recently

mixed 3d/4f metal aggregates,^[4] low-nuclearity 4f metal complexes,^[5] and even mononuclear complexes (called single-ion magnets, SIMs) of lanthanide,^[6] actinide,^[7] and transition-metal ions^[8] have been reported to exhibit slow relaxation of the magnetization.

It should be noted that for integer-spin systems with $D < 0$ fast quantum tunneling of the magnetization (QTM) through the mixing of $\pm Ms$ levels may suppress the observation of slow magnetic relaxation through a thermally activated mechanism. QTM is promoted by transverse zero-field splitting (E), hyperfine interactions, and/or dipolar interactions.^[1] The application of a small direct current (dc) field, stabilizing the negative Ms levels with regard to the positive ones, may remove the degeneracy of the $\pm Ms$ levels on either side of the energy barrier, tilting the system out of resonance and, on occasion, enabling the thermally activated mechanism. For non-integer spin systems with $D < 0$, the mixing of the degenerate ground state $\pm Ms$ levels through transverse anisotropy (E) is forbidden, thus favoring observation of the thermally activated relaxation process.^[9] This situation, together with the fact that mononuclear species can exhibit larger anisotropies than their multinuclear counterparts (the

[*] Prof. E. Colacio, Dr. J. Ruiz
Departamento de Química Inorgánica, Facultad de Ciencias
Universidad de Granada
Avda de Fuentenueva s/n, 18071 Granada (Spain)
E-mail: ecolacio@ugr.es

Prof. E. Ruiz, E. Cremades
Departament de Química Inorgànica and Institut de Recerca de
Química Teòrica i Computacional, Universitat de Barcelona
Diagonal 645, 08028 Barcelona (Spain)

Dr. J. Krzystek
National High Magnetic Field Laboratory
Florida State University, Tallahassee, FL 32310 (USA)

Prof. S. Carretta
Dipartimento di Fisica e Scienze della terra, Università de Parma
and Unità CNISM di Parma
43124 Parma (Italy)

Dr. J. Cano
Institut de Ciencia Molecular (ICMOL) and Fundació General de la
Universitat de València (FGUV), Universitat de València
46980 Paterna, València (Spain)

Dr. T. Guidi
ISIS Facility, Rutherford Appleton Laboratory
Chilton, Didcot, Oxon OX11 0QX (UK)

Dr. W. Wernsdorfer
Institut Néel-CNRS
38042 Grenoble (France)

Prof. E. K. Brechin
EaStCHEM School of Chemistry
The University of Edinburgh
West Mains Road, Edinburgh, EH9 3JJ (UK)
E-mail: ebrechin@staffmail.ed.ac.uk

[**] This work was supported by the MINECO (Spain) (Project CTQ2011-24478), the Junta de Andalucía (FQM-195 and Project of excellence P08-FQM-03705), and the University of Granada. E.R. and E.C. thank MINECO grant No. CTQ2011-23862-C02-01 and Generalitat de Catalunya grant No. 2009SGR-1459, for financial support. We would like to thank Prof. Liviu Chibotaru for providing us the SINGLE_ANISO program and Dr. Andrew Ozarowski for the EPR simulation software. E.K.B. thanks the EPSRC and Leverhulme Trust for financial support. The NHMFL is funded by the NSF, DoE, and the state of Florida. J.C. acknowledges financial support by the Spanish Ministerio de Ciencia e Innovación through projects CTQ2010-15364, Molecular Nanoscience (Consolider Ingenio CSD2007-00010), and Generalitat Valenciana (PROMETEO/2009/108). W.W. acknowledges the ARN-PNANO project MolNanoSpin No. ANR-08-NANO-002 and the ERC Advanced Grant MolNanoSpin No. 226558. J.K. acknowledges NSF grant DMR 1157490.

Supporting information for this article is available on the WWW under <http://dx.doi.org/10.1002/anie.201304386>.

control of the total anisotropy in polynuclear systems is extremely difficult), has prompted the search for SMMs based on mononuclear Co^{II} complexes with an $S = 3/2$ ground state. Results in this field are limited to nine examples with pseudotetrahedral, square-pyramidal, rhombic octahedral, or triangular prismatic geometries,^[8a–g] two of which display easy-plane anisotropy ($D > 0$). For Co^{II} systems with $D > 0$, the direct spin-phonon relaxation process between the $M_S = \pm 1/2$ ground Kramers doublet is forbidden in zero field. When $D \gg g\mu_B H$ the transition becomes allowed as the applied magnetic field induces mixing with the excited $M_S = \pm 3/2$ Kramers doublet, but with a small probability.

In principle, therefore, it is indeed possible for slow relaxation to occur in complexes where $D > 0$. In fact, it has been shown recently that two mononuclear Co^{II} complexes with a significant easy-plane $D > 0$ anisotropy, are able to exhibit slow relaxation of the magnetization.^[8a,d] This was explained in one case as being due to a field-induced bottleneck process,^[8a] and the presence of a transverse anisotropy barrier governed by E in the other.^[8d] Nevertheless, the origin of SIM properties in mononuclear Co^{II} complexes with $D > 0$ remains rather unclear and more examples of this type of compound are needed to shed light on the subject. With these ideas in mind, we have prepared a Co^{II}–Y^{III} SIM with the compartmental ligand N,N',N'' -trimethyl- N,N' -bis(2-hydroxy-3-methoxy-5-methylbenzyl)-diethylenetriamine (H_2L , Figure 1), in which the Co^{II} ion is

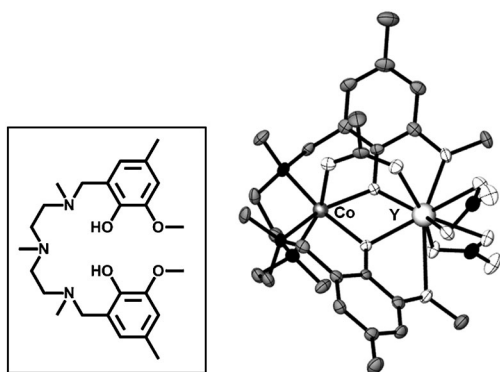


Figure 1. The structure of the ligand H_2L (inset) and a perspective view of the structure of **1**. N black, O white, C = gray. Hydrogen atoms have been omitted for clarity.

forced to adopt a CoN_3O_3 trigonally distorted octahedral coordination sphere in the inner site of the L^{2-} ligand.

The reaction of H_2L with $Co(OAc)_2 \cdot 4H_2O$ and subsequently with $Y(NO_3)_3 \cdot 6H_2O$ in MeOH in 1:1:1 molar ratio led to pink crystals of the compound $[Co(\mu-L)(\mu-OAc)Y(NO_3)_2]$ (**1**; see the Supporting Information for full experimental details). The structure of **1** (Figure 1) is very similar to those previously reported by us for other 3d–4f analogues,^[10] and consists of isolated $[Co(\mu-L)(\mu-OAc)Y(NO_3)_2]$ molecules in which the Co^{II} and Y^{III} ions are bridged by two phenoxo groups of the L^{2-} ligand and one *syn-syn* acetate anion.

The Co^{II} ion has a trigonally distorted octahedral CoN_3O_3 coordination polyhedron, where the three N atoms from the

amine groups, and consequently the three O atoms belonging to the acetate and phenoxo bridging groups, occupy *fac* positions. The distortion takes place along the three-fold axis passing through the N_3 and O_3 faces of the octahedron. Calculation of the degree of distortion of the Co^{II} coordination polyhedron with respect to an ideal six-vertex polyhedron using continuous shape measure theory and SHAPE software,^[11] led to shape measures relative to the octahedron (OC-6) and trigonal prism (TPR-6) with values of 2.8 and 8.4, respectively. A zero value corresponds to an ideal polyhedron. The shape measures relative to other reference polyhedra are significantly larger and therefore the CoN_3O_3 coordination sphere of **1** is found in the OC-6 ↔ TPR-6 deformation pathway, but closer to octahedral geometry (ca. 60%). The Y^{III} ion exhibits a rather asymmetric YO_6 coordination sphere, consisting of the two phenoxo bridging oxygen atoms, the two methoxy oxygen atoms, one oxygen atom from the acetate bridging group and four oxygen atoms belonging to two bidentate nitrate anions. The bridging acetate group forces the structure to be folded with a hinge angle of the $M(\mu-O_2)Y$ bridging fragment of 21.3° ; the hinge angle, β , being the dihedral angle between the O–Co–O and O–Y–O planes in the bridging fragment.

The $\chi_M T$ value for **1** at room temperature ($2.94 \text{ cm}^3 \text{ mol}^{-1} \text{ K}$) is significantly larger than the spin-only value for a high-spin Co^{II} ion ($S = 3/2$, $1.875 \text{ cm}^3 \text{ mol}^{-1} \text{ K}$ with $g = 2$), which is indicative of the unquenched orbital contribution of the Co^{II} ion in distorted octahedral geometry (Figure S1). The $\chi_M T$ product remains almost constant from room temperature to 70 K and then slightly decreases reaching a value of $1.96 \text{ cm}^3 \text{ mol}^{-1} \text{ K}$ at 2 K. Because the molecules are well isolated in the crystal, this decrease is most likely due to spin-orbit coupling (SOC) effects rather than intermolecular antiferromagnetic interactions. The magnetic susceptibility data for **1** were analyzed by introducing SOC effects through the Hamiltonian [Eq. (1)]:

$$\hat{H} = \alpha \hat{L} \cdot \hat{S} + \Delta [\hat{L}_z^2 - \hat{L}(\hat{L} + 1)/3] + \delta (\hat{L}_x^2 - \hat{L}_y^2) + \beta H (-\alpha \hat{L} + g_e \hat{S}) \quad (1)$$

where λ is the spin-orbit coupling parameter, α is the orbital reduction factor, and Δ and δ are the axial and rhombic orbital splitting of the T_1 term (Figure S2). Using the VPMAG package,^[12] the best-fit was found with the values $\lambda = -109.2 \text{ cm}^{-1}$, $\alpha = 1.421$, $\Delta = 645.5 \text{ cm}^{-1}$, and $\delta = -55.8 \text{ cm}^{-1}$, with an agreement factor $R = 2.3 \times 10^{-6}$. The order of energies of the 3d orbitals obtained from complete active space (CAS) calculations (see the Supporting Information for a detailed discussion) unambiguously supports the sign of Δ . Moreover, the magnitude of the calculated Δ value is close to the experimental value.

When Δ is large enough and positive, as in this case, only the two lowest Kramers doublets arising from the 4A_2 ground term, are thermally populated and the energy gap between them can be considered as an axial zero-field splitting (ZFS) within the quartet state. The magnetic properties can then be analyzed by using the Hamiltonian $\mathbf{H} = D[\mathbf{S}_z^2 - \mathbf{S}(\mathbf{S} + 1)/3] + E(\mathbf{S}_x^2 - \mathbf{S}_y^2) + g\mu_B H S$

where S is the spin ground state, D and E are the axial and transverse magnetic anisotropies, respectively, μ_B is the Bohr magneton and H the applied magnetic field. If $E = 0$, then $2D$ accounts for the energy separation between $\pm 1/2$ and $\pm 3/2$ doublets arising from second-order SOC from the quartet ground state of the distorted octahedral Co^{II} ion (Figure S2). If $D > 0$ the $M_s = \pm 1/2$ doublet is below the $M_s = \pm 3/2$ doublet. The M versus H/T plots for **1** are not superimposed on a single master curve, supporting the presence of significant magnetic anisotropy. The susceptibility and magnetization data at different fields (0–5 T) and temperatures (2–5 K) were analyzed simultaneously using the VPMAG program and the above Hamiltonian (Figure S4). The best fit of the data led to the following parameters: $D = +41.7 \text{ cm}^{-1}$, $E = 1.6 \text{ cm}^{-1}$, and $g = 2.50$ with $R = 1.4 \times 10^{-5}$, indicating the existence of significant easy-plane anisotropy in **1**. However, a good fit was also found with $D = +47 \text{ cm}^{-1}$, $E = 2.0 \text{ cm}^{-1}$, and $g = 2.503$ ($R = 2.1 \times 10^{-4}$). Accordingly, the separation between the $M_s = \pm 1/2$ and $M_s = \pm 3/2$ doublets should be in the range $83.6\text{--}94.3 \text{ cm}^{-1}$. Because of the large positive D value, the system can be considered as a doublet at low temperature rather than a quartet, and the magnetization data were analyzed in this way affording an effective g value, $g_{\text{eff}} = 4.63$.

Inelastic neutron scattering (INS) experiments were performed using the LET time-of-flight spectrometer^[13] at the ISIS spallation neutron source. Measurements were performed with an incident energy of 22 meV, giving a resolution of 0.9 meV at the elastic line. The data collected at 4 K and 100 K, corrected for the Bose factor, are shown in Figure 2. A magnetic peak is clearly observed at 11.8 meV

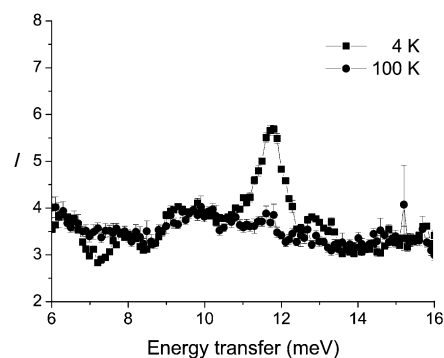


Figure 2. Temperature dependence of the INS spectra measured on LET with an incident energy of 22 meV. The data have been corrected for the Bose factor.

(95.2 cm^{-1}), which corresponds to a transition from the $M_s = \pm 1/2$ to $M_s = \pm 3/2$ Kramers doublet. This energy gap is in full agreement with the values extracted from magnetic data and theoretical calculations (see below).

X-band EPR at low temperature produced rhombic spectra ($g_{\text{eff}} = [6.70, 3.62, 2.00]$ Figure S5) that are typical of an orbitally non-degenerate ground state with a large D value. Although we did not expect to observe inter-Kramers transitions which would allow us to independently determine its value (owing to the magnitude of D), we performed high-

frequency and -field EPR (HF-EPR) measurements in the 50–650 GHz, and 0–14.5 Tesla range, respectively, to confirm its sign. Indeed, the resulting low temperature spectra (down to 5 K, Figure S6) can only be interpreted as resulting from intra-Kramers transitions within the $M_s = \pm 1/2$ multiplet, as can the field versus frequency dependence of the observed turning points (Figure S7). This result shows beyond doubt that the $M_s = \pm 1/2$ multiplet lies lower on the energy scale than the $M_s = \pm 3/2$ one, hence D is positive. The rhombicity factor is estimated to be contained between the limits $0 < E/D < 0.1$ in good agreement with the magnetic results.

From CASSCF-RASSI calculations (see the Supporting Information for full details) using the whole complex it is possible to extract the following effective g values for the ground Kramers doublet: [6.72, 3.59, 2.01] and an energy gap between the $M_s = \pm 1/2$ and $M_s = \pm 3/2$ doublets of 133.6 cm^{-1} , which is in good agreement with the experimental values. The theoretical (4.55) and experimental (4.54) average g values are in agreement with the effective value obtained from the magnetization curves (4.63). Moreover, similar CASSCF-RASSI calculations using a model Co^{II} complex also provided a large positive D value ($D = +54.5 \text{ cm}^{-1}$) with a significant rhombicity ($E/D = 0.189$), and an energy gap between the $M_s = \pm 1/2$ and $M_s = \pm 3/2$ doublets of 114.7 cm^{-1} .

Dynamic alternating current (ac) magnetic susceptibility measurements as a function of temperature and frequency (Figure S11–S14) were performed on a microcrystalline powder sample of **1**.

Under zero applied dc field, no out-of-phase (χ''_{M}) signal was observed at 2 K. This may be due to fast resonant zero-field quantum tunneling of the magnetization (QTM) through degenerate energy levels. This QTM relaxation process is forbidden for Kramers doublets (the zero-field tunnel splitting is zero), but could be turned on by dipolar effects and coupling with the nuclear spin of the Co ion whose unique natural isotope has $I = 7/2$. The latter coupling scenario would lead to a tunnel splitting in the coupled states of the electronic and nuclear spins. However, when the ac measurements were performed in the presence of a small external dc field of 1000 Oe, compound **1** shows typical SMM behavior below 5 K (Figure S11–13). This field was chosen because it induces the slowest relaxation (the maximum appears at a minimum frequency of 40 Hz, see Figure S14). Even at this field, a non-negligible fast tunneling relaxation is observed at low temperatures, as indicated by the divergence in χ''_{M} below the maxima in the χ''_{M} versus T plot at different frequencies. The Cole–Cole diagrams in the temperature range 3.75–5 K (Figure S15) exhibit semi-circular shapes and can be fitted using the generalized Debye model, affording α values (this parameter determines the width of the distribution of relaxation times, so that $\alpha = 1$ corresponds to an infinitely wide distribution of relaxation times, whereas $\alpha = 0$ represents a relaxation with a single time constant) in the range 0.008–0.09, which support the existence of a single relaxation process. The set χ_0 (isothermal susceptibility), χ_S (adiabatic susceptibility), and α obtained in the above fits were further used to fit the frequency dependence of χ''_{M} at each temperature to the generalized Debye model, which permits the

relaxation time τ to be extracted. The results were then used in constructing the Arrhenius plot shown in the inset of Figure S13. The fit of the linear portion of the data afforded an effective energy barrier for the reversal of the magnetization of 22.6 K (15.7 cm⁻¹) and $\tau_0 = 8.9 \times 10^{-7}$ s. These values are similar to those found for the limited number of Co^{II} SIMs (with $D > 0$) already reported.^[8] Note that ac susceptibility studies on a magnetically dilute sample **1'** (Figure S16, S17), which was prepared through crystallization of the diamagnetic Zn–Y analogue of **1** using a Co/Zn molar ratio of 1:10 (the amount of **1** present in the dilute sample was determined to be 11% from the low-temperature portions of the dc susceptibility for the dilute and the neat compound), show that **1'** does not show slow relaxation at zero field. When a field of 1000 Oe is applied to **1'** the energy barrier slightly increases to a value of 27.1 K (18.8 cm⁻¹) with $\tau_0 = 4.05 \times 10^{-7}$ s. This behavior indicates that the slow relaxation is induced by the magnetic field and is of molecular origin. For magnetic dc applied fields in the range 1000–2500 Oe the same thermal energy barriers were obtained.

To study the low-temperature behavior of complex **1**, single-crystal dc magnetization measurements were performed on a micro-SQUID in the temperature range 0.03–5 K with a field sweep rate of 0.14 T/s (Figure 3 and Fig-

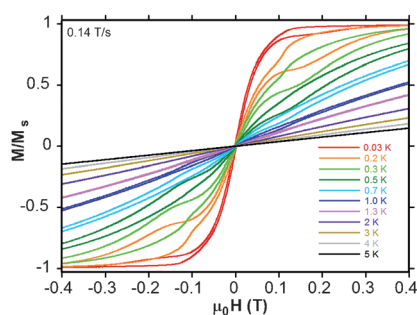


Figure 3. Field dependence of the normalized magnetization of **1** in the indicated temperature range and field sweep rate.

ure S18). The observed hysteresis loops are strongly temperature and sweep rate dependent, showing a step at zero-field. Interestingly the loops at 0.2–0.7 K are more pronounced than those at the lowest temperature, 0.03 K. At first glance this behavior may appear somewhat unusual, but in reality it is a simple reflection of the presence of fast tunnel rates, that is, when the fastest sweep rate is still too slow with respect to the tunnel rate. At the lowest temperature measured, most of the spins tunnel yielding a small hysteresis. At slightly higher temperatures thermal activation in the region of tunneling slows down the net tunnel rate because some spins relax back, and as a result, the hysteresis increases. This back relaxation is only efficient close to zero field. Notice that above 1.3 K, hysteresis is not observed.

The observation of field-induced slow relaxation in **1** is difficult to rationalize. Two other mononuclear Co^{II} complexes with $D > 0$ have been reported recently. For the first, a tetrahedral complex,^[8a] the SIM behavior was ascribed to a field-induced bottleneck of the direct relaxation in the

ground $M_S = \pm 1/2$ levels. Direct relaxation becomes so slow that an Orbach relaxation pathway is induced through the excited $M_S = \pm 3/2$ levels. The Orbach pathway is controlled by D and the thermal energy barrier extracted from ac measurements is almost equal to the difference between the $M_S = \pm 1/2$ and $M_S = \pm 3/2$ levels obtained from single-crystal EPR measurements. However, in the case of **1** this explanation does not seem to be pertinent, since 1) the dilution does not significantly increase the relaxation rate, suggesting that phonon bottleneck effects are not very important, and 2) the U_{eff} observed for **1** is significantly lower than the energy gap between the $M_S = \pm 1/2$ and $M_S = \pm 3/2$ doublets. In the second case, a rhombically distorted octahedral Co^{II} complex,^[8d] the energy barrier of 16.2 cm⁻¹ is very close to that determined for **1** and **1'**, and much smaller than that extracted from magnetization data. It was suggested that the slow relaxation in this compound arises from a transverse anisotropy barrier governed by E instead of D . However, this explanation does not seem applicable to **1** either, because it exhibits too small an E value.

The relaxation times for **1**, in the 3.75–5 K range, can be fitted to a T^{-n} law with $n = 4.5$ (Figure 4, and Figure S17). Although $n = 9$ is expected for Raman relaxation in Kramers ions,^[14] smaller n values in the range 1–6 can occur if both

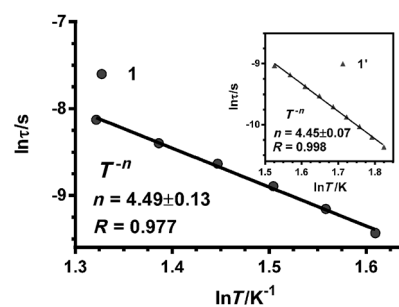


Figure 4. Power law for **1** and **1'** (inset) in the form $\ln \tau$ versus $\ln T$.

acoustic and optical phonons are considered.^[15] Interestingly, similar behavior has been found in a six-coordinate YbN₃O₃ complex,^[16] for which the relaxation times obey the T^{-n} law with $n = 2.37$. An admixture of single phonon direct processes and optical acoustic Raman-like processes has been proposed for the spin-lattice relaxation in this compound. A Raman process has also been found to significantly influence the magnetic relaxation in a recently published Co^{II}Co^{III}₃ SIM with large axial anisotropy.^[8f] In view of the above facts, it may be reasonable to speculate that an optical acoustic Raman process could also be dominant in the spin-phonon relaxation process of **1**.

The foregoing results represent an additional example of how mononuclear Co^{II} complexes with $D > 0$ can exhibit slow relaxation of the magnetization and SIM behavior. The experimental results and theoretical calculations suggest that the previously reported explanations for the spin-lattice relaxation in Co^{II} SIMs with $D > 0$ do not apply in this case and that an optical acoustic Raman process for the spin relaxation may dominate.

Received: May 21, 2013
Published online: July 14, 2013

Keywords: cobalt · N,O ligands · positive zero-field splitting · single ion magnets · yttrium

- [1] D. Gatteschi, R. Sessoli, J. Villain, *Molecular Nanomagnets*, Oxford University Press, Oxford, UK, **2006**.
- [2] a) G. Aromí, E. K. Brechin, *Struct. Bonding (Berlin)* **2006**, *122*, 1; b) R. Bagai, G. Christou, *Chem. Soc. Rev.* **2009**, *38*, 1011; c) "Molecular Magnets", themed issue (Editor: E. K. Brechin), *Dalton Trans.* **2010**.
- [3] a) W. Wernsdorfer, R. Sessoli, *Science* **1999**, *284*, 133; b) N. M. Leuenberger, D. Loss, *Nature* **2001**, *410*, 789; c) F. Meier, D. Loss, *Physica B* **2003**, *329*, 1140; d) L. Bogani, W. Wernsdorfer, *Nat. Mater.* **2008**, *7*, 179.
- [4] a) M. Andruh, J. P. Costes, C. Diaz, S. Gao, *Inorg. Chem.* **2009**, *48*, 3342; b) M. Andruh, *Chem. Commun.* **2011**, *47*, 3025; c) L. Sorace, C. Benelli, D. Gatteschi, *Chem. Soc. Rev.* **2011**, *40*, 3092.
- [5] a) Y.-N. Guo, G.-F. Xu, Y. Guo, J. Tang, *Dalton Trans.* **2011**, *40*, 9953; b) R. J. Blagg, C. A. Muryn, E. J. L. McInnes, F. Tuna, R. E. P. Winpenny, *Angew. Chem.* **2011**, *123*, 6660; *Angew. Chem. Int. Ed.* **2011**, *50*, 6530; c) C.-S. Liu, M. Du, E. C. Sañudo, J. Echeverría, M. Hu, Q. Zhang, L.-M. Zhou, S.-M. Fang, *Dalton Trans.* **2011**, *40*, 9366; d) J. D. Rinehart, M. Fang, W. J. Evans, J. R. Long, *Nat. Chem.* **2011**, *3*, 538; e) J. D. Rinehart, M. Fang, W. J. Evans, J. R. Long, *J. Am. Chem. Soc.* **2011**, *133*, 14236.
- [6] a) S. Takamatsu, T. Ishikawa, S.-Y. Koshihara, N. Ishikawa, *Inorg. Chem.* **2007**, *46*, 7250; b) M. A. Aldamen, S. Cardona-Serra, J. M. Clemente-Juan, E. Coronado, A. Gaita-Ariño, C. Martí-Gastaldo, F. Luis, O. Montero, *Inorg. Chem.* **2009**, *48*, 3467; c) D.-P. Li, T.-W. Wang, C.-H. Li, D.-S. Liu, Y.-Z. Li, X.-Z. You, *Chem. Commun.* **2010**, *46*, 2929; d) Y. Bi, Y.-N. Guo, L. Zhao, Y. Guo, S.-Y. Lin, S. D. Jiang, J. Tang, B. W. Wang, S. Gao, *Chem. Eur. J.* **2011**, *17*, 12476; e) G.-J. Chen, Y.-N. Guo, J.-L. Tian, J. Tang, W. Gu, X. Liu, S. P. Yan, P. Cheng, D.-Z. Liao, *Chem. Eur. J.* **2012**, *18*, 2484; f) A. Yamashita, A. Watanabe, S. Akine, T. Nabeshima, M. Nakano, T. Yamamura, T. Kajiwara, *Angew. Chem.* **2011**, *123*, 4102; *Angew. Chem. Int. Ed.* **2011**, *50*, 4016; g) H. L. C. Feltham, Y. Lan, F. Klöwer, L. Ungur, L. F. Chibotaru, A. K. Powell, S. Brooker, *Chem. Eur. J.* **2011**, *17*, 4362; h) G. Cucinotta, M. Perfetti, J. Luzon, M. Etienne, P.-E. Car, A. Caneschi, G. Calvez, K. Bernot, R. Sessoli, *Angew. Chem.* **2012**, *124*, 1638; *Angew. Chem. Int. Ed.* **2012**, *51*, 1606; i) S. D. Jiang, S.-S. Liu, L.-N. Zhou, B. W. Wang, Z. M. Wang, S. Gao, *Inorg. Chem.* **2012**, *51*, 3079; j) K. R. Meihaus, J. R. Rinehart, J. R. Long, *Inorg. Chem.* **2011**, *50*, 8484; k) J. Ruiz, A. J. Mota, A. Rodríguez-Diéguez, S. Titos, J. M. Herrera, E. Ruiz, E. Cremades, J. P. Costes, E. Colacio, *Chem. Commun.* **2012**, *48*, 7916.
- [7] Ref. [6j] and references therein.
- [8] a) J. R. Long, *Chem. Commun.* **2012**, *48*, 3897; b) T. Jurca, A. Farghal, P.-H. Lin, I. Korobkov, M. Murugesu, D. S. Richardson, *J. Am. Chem. Soc.* **2011**, *133*, 15814; c) J. M. Zadrozny, J. R. Long, *J. Am. Chem. Soc.* **2011**, *133*, 20732; d) J. Vallejo, I. Catro, R. Ruiz-Gracia, J. Cano, M. Julve, F. Lloret, G. DeMunno, W. Wernsdorfer, E. Pardo, *J. Am. Chem. Soc.* **2012**, *134*, 15704; e) A. Buchholz, A. O. Eseola, W. Plass, *C. R. Chim.* **2012**, *15*, 929; f) E. Colacio, *Inorg. Chem.* **2013**, *52*, 4554; g) Y.-Y. Zhu, C. Cui, Y.-Q. Zhang, J.-H. Jia, X. Guo, C. Gao, K. Qian, S.-D. Jiang, B.-W. Wang, Z.-M. Wang, S. Gao, *Chem. Sci.* **2013**, *4*, 1802; h) D. E. Freedman, W. H. Harman, T. D. Harris, G. J. Long, C. J. Chang, J. R. Long, *J. Am. Chem. Soc.* **2010**, *132*, 1224; i) W. H. Harman, T. D. Harris, D. Freedman, E. H. Fong, A. Chang, J. D. Rinehart, A. Ozarowski, M. T. Sougrati, F. Grandjean, G. J. Long, J. R. Long, *J. Am. Chem. Soc.* **2010**, *132*, 18115; j) D. Weismann, Y. Sun, Y. Lan, G. Wolmershäuser, A. K. Powell, H. Sitzmann, *Chem. Eur. J.* **2011**, *17*, 4700; k) P.-H. Lin, C. N. Smythe, J. S. Gorelsky, S. Maguire, J. N. Henson, I. Korobkov, L. B. Scott, C. J. Gordon, T. Baker, M. Murugesu, *J. Am. Chem. Soc.* **2011**, *133*, 15806; l) S. Mossin, B. L. Tran, D. Adhikari, M. Pink, F. W. Heinemann, J. Sutter, R. K. Szilayi, K. Meyer, D. J. Mindiola, *J. Am. Chem. Soc.* **2012**, *134*, 13651; m) J. M. Zadrozny, M. Atanasov, A. M. Bryan, C.-Y. Lin, B. D. Reinken, P. P. Power, F. Neese, J. R. Long, *Chem. Sci.* **2013**, *4*, 125; n) M. Atanasov, J. M. Zadrozny, J. F. Long, F. Neese, *Chem. Sci.* **2013**, *4*, 139.
- [9] H. A. Kramers, *Proc. R. Acad. Sci. Amsterdam* **1930**, *33*, 959.
- [10] a) E. Colacio, J. Ruiz-Sanchez, F. J. White, E. K. Brechin, *Inorg. Chem.* **2011**, *50*, 7268; b) E. Colacio, J. Ruiz, A. J. Mota, M. A. Palacios, E. Cremades, E. Ruiz, F. J. White, E. K. Brechin, *Inorg. Chem.* **2012**, *51*, 5857.
- [11] M. Llunell, D. Casanova, J. Cirera, J. M. Bofill, P. Alemany, S. Alvarez, M. Pinsky, D. Avnir, SHAPE v1.1b, Barcelona, **2005**.
- [12] J. Cano, VPMAG package, University of Valencia, Valencia, Spain, **2003**.
- [13] R. I. Bewley, J. W. Taylor, S. M. Bennington, *Nucl. Instrum. Methods Phys. Res.* **2011**, *637*, 128.
- [14] A. Abragam, B. Bleaney, *Electron Paramagnetic Resonance of Transition Ions*, Clarendon, Oxford, **1970**.
- [15] K. N. Shrivastava, *Phys. Status Solidi B* **1983**, *117*, 437.
- [16] J.-L. Liu, K. Yuan, J.-D. Leng, L. Ungur, W. Wernsdorfer, F.-S. Guo, L. F. Chibotaru, M.-L. Tong, *Inorg. Chem.* **2012**, *51*, 8538.